Computers and Mathematics with Applications 61 (2011) 1475–1492

Contents lists available at ScienceDirect

Computers and Mathematics with Applications

journal homepage: www.elsevier.com/locate/camwa

A fitted numerical method for a system of partial delay differential equations☆

Eihab B.M. Bashier, Kailash C. Patidar*

Department of Mathematics and Applied Mathematics, University of the Western Cape, South Africa

ARTICLE INFO

Article history:
Received 27 March 2009
Received in revised form 5 October 2010
Accepted 5 November 2010

Keywords:
System of partial delay differential equations
Ecological models
Bifurcation analysis
Method of lines
Fitted operator finite difference method
Convergence analysis

ABSTRACT

We consider a system of two coupled partial delay differential equations (PDDEs) describing the dynamics of two cooperative species. The original system is reduced to a system of ordinary delay differential equations (DDEs) obtained by applying the method of lines. Then we construct a fitted operator finite difference method (FOFDM) to solve this resulting system. The model considered in this paper is very sensitive to small changes in the parameters associated in with the model. Depending on the values of these parameters, the solution can be stable, periodic and/or aperiodic. Such behavior of the solution is exploited via the proposed FOFDM. This FOFDM is analyzed for convergence and it is seen that this method is unconditionally stable and has the accuracy of $\mathcal{O}(k+h^2)$, where k and h denote time and space step-sizes, respectively. Some numerical results confirming theoretical observations are also presented. These results are comparable with those obtained in the literature.

1. Introduction

We consider the following system of two coupled PDDEs describing the dynamics of two cooperative species with densities $u(t,x)$ and $v(t,x)$:

$$\frac{\partial u}{\partial t}(t,x) = \lambda_1 \frac{\partial^2 u}{\partial x^2}(t,x) + u(t,x)(r_1 - a_{11}u(t-\tau,x) + a_{12}v(t-\tau,x)) \tag{1.1}$$

$$\frac{\partial v}{\partial t}(t,x) = \lambda_2 \frac{\partial^2 v}{\partial x^2}(t,x) + v(t,x)(r_2 + a_{21}u(t-\tau,x) - a_{22}v(t-\tau,x)) \tag{1.2}$$

where $0 < x < \pi$ and $t > 0$, subject to the initial data

$$u(t,x) = u^0(t,x), \qquad v(t,x) = v^0(t,x), \quad t \in [-\tau, 0], \tag{1.3}$$

and Dirichlet boundary conditions

$$u(t,0) = u(t,\pi) = v(t,0) = v(t,\pi) = 0, \quad t \geq 0. \tag{1.4}$$

The constants $\lambda_1 > 0$ and $\lambda_2 > 0$ in the above represent the diffusivity of the two species whereas constants $r_1 > 0$ and $r_2 > 0$ are the growth rates of these species. The coefficients a_{11}, a_{12}, a_{21} and a_{22} are positive constants. Finally, τ (>0) is a time delay parameter.

☆ The research contained in this report has been supported by the South African National Research Foundation.

* Corresponding address: Department of Mathematics and Applied Mathematics, University of the Western Cape, Private Bag X17, Bellville 7535, Bellville, South Africa. Tel.: +27 21 9593917; fax: +27 21 9591241.
E-mail address: kpatidar@uwc.ac.za (K.C. Patidar).

0898-1221/$ – see front matter
doi:10.1016/j.camwa.2010.11.010

Many biological phenomena can be described by diffusion equations such as the system above. Some examples include the dynamics of a single species in time and space [1], the spread of an advantageous gene in a population [2], the competition between the gray and red squirrels in Britain which led to the decline and subsequent disappearance of the red squirrels [3], the spread of powdery mildew disease caused by the fungus Uncinula necator over the grapes–vines [4], the modified Lotka–Volterra system with logistic growth of the prey and with both predator and prey dispersing by diffusion [3].

The literature on the use of diffusive delay differential equations for modeling the biological systems is very rich, see, for example [5–7] and the references therein. When a time delay is involved, it indicates the non-immediate affect of some factor that inhibits the dynamics of the model. For instance, in a predator–prey model, the density of the prey is affected by hunting mature prey members that happened some time on the past. Also, in a model that describes the spread of an epidemic disease, a virus or a bacterium takes some time before it becomes mature and be able to attack some organism. In a biological system, delay models are more realistic for describing the dynamics of the various parts of the system than the ordinary differential equations.

Under the assumption that the two species have the same diffusivity (i.e., $\lambda_1 = \lambda_2 = \lambda$) and same growth rates (i.e., $r_1 = r_2 = r$), Li et al. [8] used a transformation of variables to reduce the system (1.1)–(1.2) to the form

$$\frac{\partial u}{\partial t}(t,x) = \lambda \frac{\partial^2 u}{\partial x^2}(t,x) + \kappa u(t,x)(1 - u(t-\tau,x) + a_{12} v(t-\tau,x)), \tag{1.5}$$

$$\frac{\partial v}{\partial t}(t,x) = \lambda \frac{\partial^2 v}{\partial x^2}(t,x) + \kappa v(t,x)(1 + a_{21} u(t-\tau,x) - v(t-\tau,x)), \tag{1.6}$$

with $t > 0, 0 < x < \pi$ and subject to the initial data (1.3) and the boundary conditions (1.4).

The deficiencies of the standard finite difference methods in solving the problems like above are well-known. While explicit methods can solve such differential equations with low computational cost, they have the drawback that their stability regions are very small and hence severe restrictions on the time and space step-sizes will be required in order to achieve satisfactorily converging results. On the other hand, the implicit schemes do have wider stability regions but the associated computational complexity is very high and they cannot achieve more than one order as compared to explicit methods that use the same number of stages [9].

In this paper, we design a new fitted operator finite difference method (FOFDM) which is constructed for a system of DDEs obtained by applying the method of lines [10,11] to the system of PDDEs. These FOFDMs, which are based on the philosophy of non-standard finite difference methods of Mickens [12,13] are widely used for singularly perturbed two-point boundary value problems. See for instance [14–16]. However, their extensions for the coupled PDEs whose solutions possess oscillatory dynamics, have not been seen in the literature.

The rest of this paper is organized as follows. In Section 2, we discuss the existence and stability of equilibria for the model under consideration. Section 3 deals with the construction of the fitted operator finite difference method which is analyzed for convergence in Section 4. Illustrative numerical results are presented in Section 5. Finally, we discuss these results and draw some conclusions in Section 6.

2. Existence and stability of equilibria

In many of the delay differential equation models, the time delay τ acts as a bifurcation parameter. As the delay τ passes through some critical value $\tau^\star$, a couple of complex conjugating eigenvalues of the system passes the imaginary axis at some pure imaginary points and stable periodic Hopf bifurcating solutions occur. Then when τ passes $\tau^\star$, the real parts of these eigenvalues pass to the positive real axis causing the Hopf bifurcating solution to be unstable. We summarize these features of the solution via the existence and stability of a positive equilibrium following the works in [17,8,1].

Let $\tilde{\kappa}$ corresponds to the ratio κ/λ. Then, if $\tilde{\kappa} < 1$, the trivial solution

$$(u(t,x), v(t,x)) = (0,0)$$

is asymptotically stable and it is the only global attractor for all non-negative solutions. Therefore, the increase in the time delay τ does not have affect on the stability of the trivial equilibria.

On the other hand, when $\tilde{\kappa} > 1$ the trivial solution is unstable and a positive equilibrium $(U_{\tilde{\kappa}}(x), V_{\tilde{\kappa}}(x))$ will bifurcate from the trivial solution at $\tilde{\kappa} = 1$. In this case, for each fixed $0 < \tilde{\kappa} - 1 \ll 1$ when the delay parameter τ increases, it passes through a sequence $\{\tau_{\tilde{\kappa}_n}\}_{n=0}^{\infty}$ of critical delay. When $\tau = \tau_{\tilde{\kappa}_n}, n = 0, 1, \ldots$ a bifurcation occurs and the positive equilibrium $(U_{\tilde{\kappa}}, V_{\tilde{\kappa}})$ is asymptotically stable for $\tau < \tau_{\tilde{\kappa}_0}$ and unstable for $\tau > \tau_{\tilde{\kappa}_0}$. Moreover, the bifurcating solutions which occur from the Hopf bifurcation point $\tau = \tau_{\tilde{\kappa}_0}$ are stable while those occurring from the Hopf bifurcation points $\tau = \tau_{\tilde{\kappa}_n}, n = 1, 2, \ldots$ are unstable.

In summary,

- If $\tilde{\kappa} \leq 1$, then the zero solution is stable and is the only global attractor of all non-negative solutions.
- If $\tilde{\kappa} > 1$, a unique positive equilibrium $(U_{\tilde{\kappa}}, V_{\tilde{\kappa}})$ bifurcates from $\tilde{\kappa} = 1$ and $(u, v) = (0, 0)$ while the zero solution is unstable.
- For each fixed $0 < \tilde{\kappa} - 1 \ll 1$ there exists a sequence $\{\tau_{\tilde{\kappa}_n}\}_{n=0}^{\infty}$ such that the positive equilibrium $(U_{\tilde{\kappa}}, V_{\tilde{\kappa}})$ is asymptotically stable if $0 \leq \tau < \tau_{\tilde{\kappa}_0}$ and unstable if $\tau > \tau_{\tilde{\kappa}_0}$.
- A Hopf bifurcation will occur as the delay τ increasingly passes through each point $\tau_{\tilde{\kappa}_n}, n = 1, 2, \ldots$.

3. Construction of the numerical method

In this section, we describe the construction of the fitted numerical method for solving the system (1.5)–(1.6) with the initial data (1.3) and boundary conditions (1.4) respectively. Following the method of lines, we find an approximation to the derivatives of the functions $u(t, x)$ and $v(t, x)$ with respect to the spatial variable x by algebraic quantities in purpose of transforming the two PDDEs into a system of DDEs.

Because of the similarities between the two PDEs in $u(t, x)$ and $v(t, x)$ we will describe the method for the equation in $u(t, x)$. The equation in $v(t, x)$ is dealt similarly.

Let N_x be a positive integer and be discretized the interval $[0, \pi]$ by the points

$$x_0 = 0 < x_1 < x_2 < \cdots < x_{N_x} = \pi$$

where $h = x_{m+1} - x_m = \pi/N_x$; $m = 0, 1, \ldots, N_x - 1$. Let $U_m(t) \approx u(t, x_m)$.

We approximate the second partial derivative $\frac{\partial^2 u}{\partial x^2}(t, x)$ by

$$\frac{\partial^2 u}{\partial x^2}(t, x_m) \approx \frac{U_{m+1} - 2U_m + U_{m-1}}{\phi_m^2}, \tag{3.7}$$

where

$$\phi_m = \phi_m(\kappa, \lambda, h) = \frac{2}{\rho_m} \sin \frac{\rho_m h}{2}$$

and $\rho_m = \sqrt{\kappa/\lambda}$. It is obvious that $\phi_m \to h$ as $h \to 0$. The function ϕ_m^2 in Eq. (3.7) is conventionally termed as a denominator function [18]. It can be constructed by using the theory of difference equations.

Since ρ_m is a constant value and hence the denominator function ϕ_m, we shall write ρ instead of ρ_m and ϕ instead of ϕ_m.

Eq. (1.5) with the initial data (1.3) and boundary conditions (1.4) then take the form

$$U_0(t) = 0 = U_{N_x}(t), \tag{3.8}$$

$$\frac{\mathrm{d}U_m(t)}{\mathrm{d}t} = \lambda \frac{U_{m+1} - 2U_m + U_{m-1}}{\phi^2} + \kappa U_m(t)(1 - u_m(t - \tau) + a_{12} v_m(t - \tau)), \quad m = 1, \ldots, N_x - 1, \tag{3.9}$$

with the initial data

$$u_m(\theta) = u^0(\theta, x_m), \quad \theta \in [-\tau, 0];\ m = 1, \ldots, N_x - 1, \tag{3.10}$$

where $u_m(t)$ is the exact value $u(t, x_m)$.

Now let N_t be a positive integer and $k = \frac{T}{N_t}$ where $0 < t < T$.

Discretizing the time interval $[0, T]$ through the points

$$0 = t_0 < t_1 < \cdots < t_{N_t} = T$$

where $t_{n+1} - t_n = k$, $n = 0, 1, \ldots, N_t - 1$.

We approximate the time derivative $\frac{\mathrm{d}U_m(t)}{\mathrm{d}t}$ at t_n by

$$\frac{\mathrm{d}U_m(t_n)}{\mathrm{d}t} \approx \frac{U_m^{n+1} - U_m^n}{\psi(k)}, \tag{3.11}$$

where the denominator function $\psi(k)$ is given by

$$\psi(k) = (\exp(\kappa k) - 1)/\kappa.$$

Again we see that $\psi(k) \to k$ as $k \to 0$.

Combining (3.8), (3.9) and (3.11), we have

$$\frac{U_m^{n+1} - U_m^n}{\psi(k)} = \lambda \frac{U_{m+1}^{n+1} - 2U_m^{n+1} + U_{m-1}^{n+1}}{\phi^2(h)} + \kappa U_m^n (1 - (H_u)_m^n + a_{12}(H_v)_m^n) \tag{3.12}$$

where $(H_u)_m^n \approx u(t_n - \tau, x_m)$ and $(H_v)_m^n \approx v(t_n - \tau, x_m)$, $m = 1, \ldots, N_x - 1$, $n = 0, \ldots, N_t - 1$ are the history functions corresponding to the equations in u and v.

Eq. (3.12) can further be simplified as

$$-\frac{\lambda}{\phi_m^2} U_{m-1}^{n+1} + \left(\frac{1}{\psi} + \frac{2\lambda}{\phi_m^2}\right) U_m^{n+1} - \frac{\lambda}{\phi_m^2} U_{m+1}^{n+1} = \left(\frac{1}{\psi} + \kappa(1 - (H_u)_m^n + a_{12}(H_v)_m^n)\right) U_m^n. \tag{3.13}$$

Eq. (3.13) can be written as a tridiagonal system

$$T_L U^{n+1} = \frac{1}{\psi} U^n + \kappa U^n (1 - H_u^n + a_{12} H_v^n), \tag{3.14}$$

where $U^n = [U_1^n, \ldots, U_{N_x-1}]^T$, $H_u{}^n = [(H_u)_1^n, \ldots, (H_u)_{N_x-1}^n]^T$, $H_v{}^n = [(H_v)_1^n, \ldots, (H_v)_{N_x-1}^n, n = 0, \ldots, N_t - 1]^T$ and

$$T_L = \text{Tri}\left(-\frac{\lambda}{\phi^2}, \frac{1}{\psi} + \frac{2\lambda}{\phi^2}, -\frac{\lambda}{\phi^2}\right).$$

On the interval $[0, \tau]$ the delayed arguments $t_n - \tau$ belong to $[-\tau, 0]$, and therefore the delayed variable $(H_u)_m^n \approx u(t_n - \tau, x_m)$ is evaluated directly from the history functions $u^0(t, x)$ as

$$(H_u)_m^n = u^0(t_n - \tau, x_m), \tag{3.15}$$

and Eq. (3.14) becomes of the form

$$T_L U^{n+1} = \frac{1}{\psi} U^n + \kappa U^n (1 - \varphi^0(t_n - \tau) + a_{12} \vartheta^0(t_n - \tau)), \tag{3.16}$$

where $\varphi^0(t_n - \tau) = [u^0(t_n - \tau, x_1), \ldots, u^0(t_n - \tau, x_{N_x-1})]^T$ and $\vartheta^0(t_n - \tau) = [v^0(t_n - \tau, x_1), \ldots, v^0(t_n - \tau, x_{N_x-1})]^T$.

Let s be the largest integer such that $t_s \le \tau$. By using Eq. (3.16) we can compute U_m^n for $1 \le n \le s$. Up to this stage, we interpolate the data

$$(t_0, U_m^0), (t_1, U_m^1), \ldots, (t_s, U_m^s)$$

using an interpolating cubic Hermite spline $\varphi_m(t)$. Then $U_m^n = \varphi(t_n, x_m)$ for all $n = 0, 1, \ldots, s$ and $m = 1, 2, \ldots, N_x - 1$.

For $n = s+1, s+2, \ldots, N_t - 1$, when we move from level n to level $n+1$ we extend the definitions of the cubic Hermite spline $\varphi_m(t)$ to the point $(t_n + k, U_m^{n+1})$. Then the history terms $(H_u)_m^n$ can be approximated by the functions $\varphi_m(t_n - \tau)$ for $n \ge s$. That is,

$$(H_u)_m^n \approx \varphi_m(t_n - \tau),$$

and Eq. (3.14) becomes of the form

$$T_L U^{n+1} = \frac{1}{\psi} U^n + \kappa U^n (1 - \varphi(t_n - \tau) + a_{12} \vartheta(t_n - \tau)), \tag{3.17}$$

where $\varphi(t_n - \tau) = [(H_u)_1^n, \ldots, (H_u)_{N_x-1}^n]^T$ and ϑ is the set of cubic Hermite splines that interpolate the data (t_n, V_m^n).

Proceeding in the similar manner for the equation in v, we have

$$T_L V^{n+1} = \frac{1}{\psi} V^n + \kappa V^n (1 + a_{21} \varphi(t_n - \tau) - \vartheta(t_n - \tau)), \tag{3.18}$$

where $V^n = [V_1^n, \ldots, V_{N_x-1}]^T$,

$$(H_v)_m^n = \begin{cases} \vartheta^0(t_n - \tau, x_m) & t_n \le \tau \\ \vartheta_m(t_n - \tau) & t_n > \tau \end{cases}$$

along with

$$V_0(t) = 0 = V_{N_x}. \tag{3.19}$$

Our FOFDM then consists of Eqs. (3.14)–(3.18) along with (3.8) and (3.19), which can be summarized as:

$$\begin{cases} T_L U^{n+1} = \dfrac{1}{\psi} U^n + \kappa U^n (1 - H_u^n + a_{12} H_v^n), \\ T_L V^{n+1} = \dfrac{1}{\psi} V^n + \kappa V^n (1 + a_{21} H_u^n - H_v^n), \end{cases} \tag{3.20}$$

where

$$\begin{cases} (H_u)_m^n = \begin{cases} u^0(t_n - \tau, x_m), & t_n \in [0, \tau] \\ \varphi_m(t_n - \tau), & t_n \in (\tau, T] \end{cases} \\ (H_v)_m^n = \begin{cases} v^0(t_n - \tau, x_m), & t_n \in [0, \tau] \\ \vartheta_m(t_n - \tau), & t_n \in (\tau, T]. \end{cases} \end{cases} \tag{3.21}$$

This method is analyzed for convergence in the next section whereas the corresponding numerical results are presented in Section 5.

4. Analysis of convergence

As usual with most of the classical convergence finite difference methods, the convergence for the proposed FOFDM is proved via consistency and stability.

4.1. Consistency of the FOFDM

We assume that the function $u(t,x)$ and its partial derivatives with respect to both t and x are smooth and satisfy

$$\left|\frac{\partial^{i+j}u(t,x)}{\partial t^i x^j}\right| \le C; \quad \forall i,j \ge 0, \tag{4.22}$$

where C is a constant that is independent of the time and space step-sizes.

The local truncation error (LTE) for the discrete equations in u in the FOFDM (3.16) and (3.17) is given by

$$(\mathrm{LTE})_u = u_t(t_n,x_m) - \frac{u_m^{n+1}-u_m^n}{\psi} - \lambda\left(u_{xx} - \frac{u_{m-1}^{n+1}-2u_m^{n+1}+u_{m+1}^{n+1}}{\phi_m^2}\right). \tag{4.23}$$

The first term on the right-hand side of Eq. (4.23) satisfies

$$\begin{aligned}
\left|u_t(t_n,x_m) - \frac{u_m^{n+1}-u_m^n}{\psi}\right| &= \left|u_t(t_n,x_m) - \frac{u_m^{n+1}-u_m^n}{k} + \frac{u_m^{n+1}-u_m^n}{k} - \frac{u_m^{n+1}-u_m^n}{\psi}\right| \\
&\le \left|u_t(t_n,x_m) - \frac{u_m^{n+1}-u_m^n}{k}\right| + \left|\frac{u_m^{n+1}-u_m^n}{k} - \frac{u_m^{n+1}-u_m^n}{\psi}\right| \\
&\le \frac{k}{2}\left|u_{tt}(\xi,x_m)\right| + \frac{\kappa k\left(\frac{1}{2}+\frac{\kappa k}{6}+\cdots\right)}{1+\frac{\kappa k}{2}+\cdots}(u_m^{n+1}-u_m^n), \quad \xi\in[t_n,t_{n+1}] \\
&\le \frac{k}{2}C + \frac{\kappa k\left(\frac{1}{2}+\frac{\kappa k}{6}+\cdots\right)}{1+\frac{\kappa k}{2}+\cdots}(u_m^{n+1}-u_m^n) \quad (\text{using (4.22)}) \\
&\to 0 \quad \text{as } k\to 0.
\end{aligned} \tag{4.24}$$

The second term of Eq. (4.23) satisfies

$$\begin{aligned}
&\left|u_{xx}(t_n,x_m) - \left(\frac{u_{m-1}^{n+1}-2u_m^{n+1}+u_{m+1}^{n+1}}{\phi^2}\right)\right| \\
&\le \left|u_{xx}(t_n,x_m) - \left(\frac{u_{m-1}^{n}-2u_m^{n}+u_{m+1}^{n}}{h^2}\right)\right| + \left|\left(\frac{u_{m-1}^{n}-2u_m^{n}+u_{m+1}^{n}}{h^2} - \frac{u_{m-1}^{n+1}-2u_m^{n+1}+u_{m+1}^{n+1}}{\phi^2}\right)\right| \\
&\le \frac{h^2}{12}\left|u_{xxxx}(t_n,\zeta)\right| + \left|\frac{(\rho h/2)^2/3-(\rho h/2)^4/60+\cdots}{1-(\rho h/2)^2/6+\cdots}\right| + k\left|u_{xxt}(\xi,x_m)\right|, \\
&\le \frac{h^2}{12}C + h^2\left(\left|\frac{(\rho/2)^2/3-h^2(\rho/2)^4/60+\cdots}{1-(\rho h/2)^2/6+\cdots}\right|\right) + kC \quad (\text{using (4.22)}), \\
&\to 0 \quad \text{as } h\to 0 \text{ and } k\to 0,
\end{aligned} \tag{4.25}$$

where $x_{m-1} < \zeta < x_{m+1}$ in the third last inequality above.

The results that we obtained in Eqs. (4.24) and (4.25) prove that LTE $\to 0$ as $k\to 0$ and $h\to 0$. Similarly, we can see that the LTE for the equation in v tends to 0, as $h\to 0$ and $k\to 0$. This proves the consistency of our FOFDM.

4.2. Stability of the FOFDM

In this section we apply the von Neumann analysis to prove the stability of our method.

For simple notation, we write $F(t,\tau,x) = 1-u(t-\tau,x)+a_{21}v(t-\tau,x)$ and $G_{\tau,m}^n = 1-U_{\tau,m}^n + a_{21}V_{\tau,m}^n$. Then, the solution function $u_\ell(t-\tau,x) = T_\ell(t)X_\ell(x)$ is bounded as

$$|u_\ell(t-\tau,x)| = |T_\ell(t)| \le \mathrm{e}^{(\kappa F(t,\tau,x)-\lambda\ell^2)t} \le \mathrm{e}^{\kappa F(t,\tau,x)T}.$$

Plugging the solution

$$U_m^n = w_n \mathrm{e}^{imh},$$

where $i = \sqrt{-1}$ in Eq. (3.14), we obtain

$$\left(\left(\frac{1}{\psi} + \frac{2\lambda}{\phi^2}\right) - \frac{\lambda}{\phi^2}\left(e^{ih} + e^{-ih}\right)\right) w_{n+1} = \left(\frac{1}{\psi} + \kappa\left(1 - U^n_{\tau,m} + a_{21}V^n_{\tau,m}\right)\right) w_n. \tag{4.26}$$

From Eq. (4.26), the amplification factor ς is given by

$$\varsigma = \frac{\frac{1}{\psi} + \kappa G^n_{\tau,m}}{\frac{1}{\psi} + \frac{4\lambda}{\phi_m^2}\sin^2\frac{h}{2}}. \tag{4.27}$$

Eq. (4.26) can be rewritten as

$$w_n = \varsigma^n w_0.$$

Now the amplification factor ς given in Eq. (4.27) must satisfy the inequality

$$|\varsigma^n| \le e^{\kappa G^n_{\tau,m} T} = e^{kN\kappa G^n_{\tau,m}},$$

yielding

$$|\varsigma| \le e^{\frac{k\kappa G^n_{\tau,m} N}{n}}. \tag{4.28}$$

The minimum value for the right-hand side of Eq. (4.28) occurs when $n = N$, therefore, we bound the left-hand side of Eq. (4.28) by $e^{k\kappa G^n_{\tau,m}}$.

Eq. (4.26) now becomes

$$\frac{\frac{1}{\psi} + \kappa G^n_{\tau,m}}{\frac{1}{\psi} + \frac{4\lambda}{\phi_m^2}\sin^2\frac{h}{2}} \le e^{k\kappa G^n_{\tau,m}}. \tag{4.29}$$

Multiplying both the numerator and denominator of the left-hand side of Eq. (4.29) by ψ yields

$$\frac{1 + \kappa\psi G^n_{\tau,m}}{1 + \frac{4\lambda\psi}{\phi_m^2}\sin^2\frac{h}{2}} \le e^{k\kappa G^n_{\tau,m}}. \tag{4.30}$$

As $n \to \infty$, $\psi \to k$ and the left-hand side of Eq. (4.30) satisfies the inequality

$$\frac{1 + \kappa\psi G^n_{\tau,m}}{1 + \frac{4\lambda\psi}{\phi_m^2}\sin^2\frac{h}{2}} \approx \frac{1 + k\kappa G^n_{\tau,m}}{1 + \frac{4k\lambda}{\phi_m^2}\sin^2\frac{h}{2}} < 1 + k\kappa G^n_{\tau,m} < e^{k\kappa G^n_{\tau,m}} \tag{4.31}$$

for any choice of denominator functions ψ and ϕ. This proves that the proposed FOFDM is unconditionally stable.

Using the Lax–Richtmyer theory [19,20], we have the following theorem.

Theorem 4.1. *The FOFDM given by (3.20)–(3.21) is convergent of order $\mathcal{O}(k + h^2)$ in the sense that*

$$\max\left\{\max_{1\le m,n\le N-1}\{|u(t_n, x_m) - U^n_m|\}, \max_{1\le m,n\le N-1}\{|v(t_n, x_m) - V^n_m|\}\right\} \le C(k + h^2),$$

where U and V are the numerical solutions obtained by this FOFDM and N is the total number of subintervals taken in either directions.

5. Numerical results

To see the performance of the proposed FOFDM, we consider the following example.

Example 5.1 (*[8]*)**.** Consider problem (1.5)–(1.6) with $a_{12} = 0.5, a_{21} = 0.8$, λ takes values in $[0.0085, 0.0105] \cup [0.999, 1.0105]$, $\kappa \in \{0.01, 1.01\}$, $\tau \in \{1, 20, 100, 170\}$ and $T \in \{100, 800, 2500, 4500\}$. The initial data is taken as

$$u(\theta, x) = v(\theta, x) = 0.1\left(1 + \frac{\theta}{\tau}\right)\sin x, \quad \theta \in [-\tau, 0],\ 0 \le x \le \pi,\ t \ge 0.$$

6. Discussion and future plans

In this paper we have designed and analyzed a fitted operator finite difference method (FOFDM) for a coupled system of two partial delay differential equations. Using the method of lines, this problem is transformed into a system of ordinary

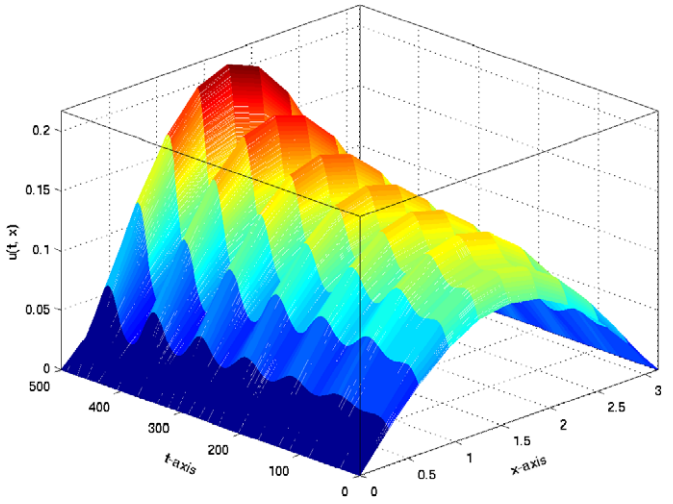

Fig. 1. Profile of $u(t, x)$ for $\lambda = 0.0096$, $\kappa = 0.01$, $\tau = 1$ and $T = 100$.

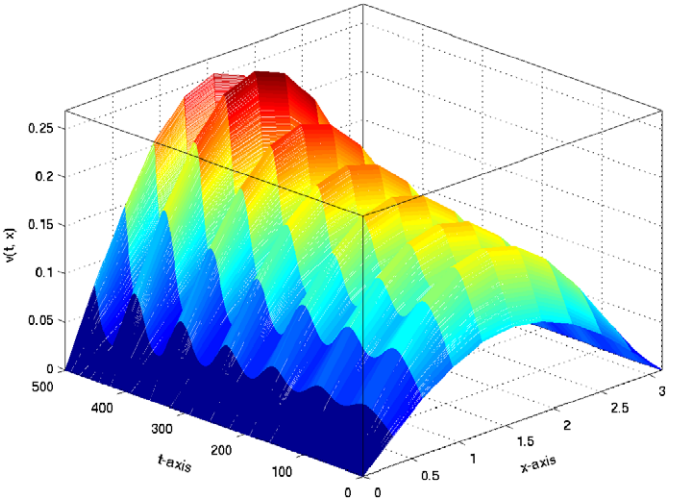

Fig. 2. Profile of $v(t, x)$ for $\lambda = 0.0096$, $\kappa = 0.01$, $\tau = 1$ and $T = 500$.

delay differential equations which are then solved with the proposed FOFDM. This FOFDM is analyzed for convergence and we found that this method is of order 1 with respect to time and is of order 2 with respect to space discretizations.

In our test example, we considered many scenarios for the selection of the parameters κ and λ such that the ratio κ/λ remains close to one. The results are presented in Figs. 1–30. We have noticed that when $\kappa/\lambda < 1$, the solutions do always go to the unique stable trivial attractor (0, 0) (see Figs. 5, 6, 13, 14, 21, 22, 29 and 30). When the ratio κ/λ passes the unity, a stable or a stable periodic solution bifurcates from $\kappa/\lambda = 1$ (see Figs. 3, 4, 9–12, 19, 20, 27 and 28). When we continue increasing the ratio κ/λ unstable periodic solutions bifurcate from $\kappa/\lambda = 1$ like what have been seen in Figs. 17, 18, 25 and 26. Finally, by increasing the ratio κ/λ more, unstable aperiodic solutions appear like what have been seen in Figs. 1, 2, 7, 8, 15, 16, 23 and 24. This confirms the theoretical results.

The results which we have obtained by fixing the value of the time delay $\tau = 100$ show that the model is very sensitive to the change in the values of the parameters. Changes in the ratio κ/λ from 0.99951 passing by 1.01 and 1.005 to 1.01101 showed four different scenarios about the behavior of the positive equilibrium. A similar situation is seen for $\tau = 170$, where changes in the ratio κ/λ from 0.99951 to 1.007 have shown four different stability scenarios for the positive equilibrium. These scenarios are the trivial equilibrium (0, 0), a stable positive equilibrium, a periodic positive equilibrium and aperiodic positive equilibrium. This again confirms the theoretical results.

In summary, from the results that we have obtained by our simulations, we conclude that for a fixed $\tau > \tau_{\kappa_0} > 0$ if

- the ratio κ/λ is less than or equal to one then the solution tends to the trivial attractor (0, 0) and the solution is stable and no positive exists.

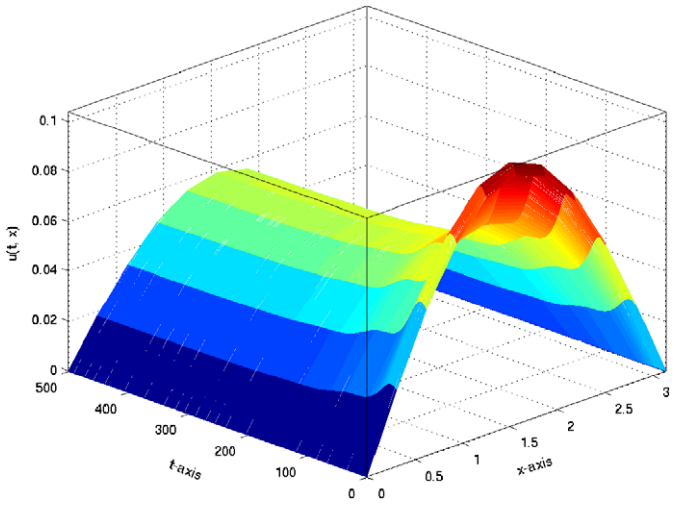

Fig. 3. Profile of $u(t, x)$ for $\lambda = 0.0098$, $\kappa = 0.01$, $\tau = 1$ and $T = 500$.

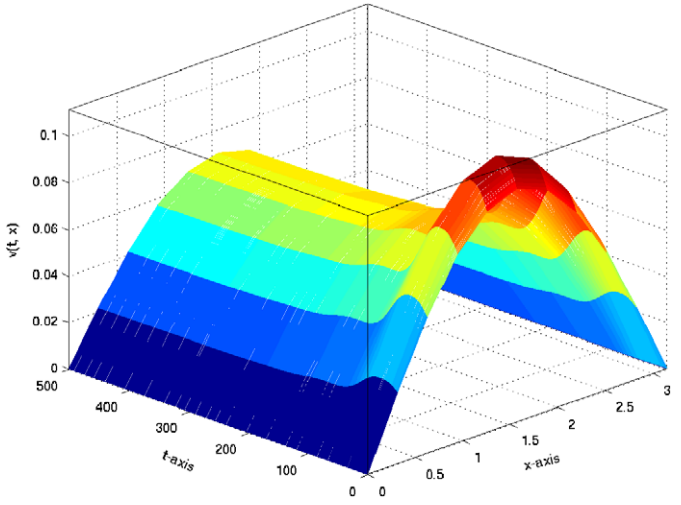

Fig. 4. Profile of $v(t, x)$ for $\lambda = 0.0098$, $\kappa = 0.01$, $\tau = 1$ and $T = 500$.

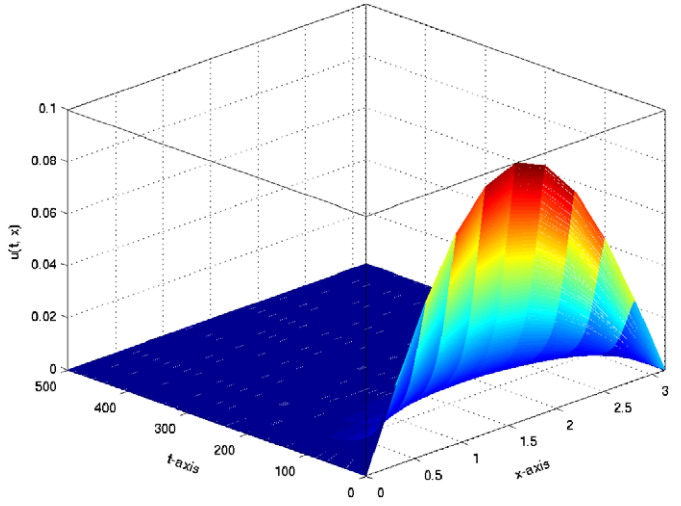

Fig. 5. Profile of $u(t, x)$ for $\lambda = 0.0105$, $\kappa = 0.01$, $\tau = 1$ and $T = 500$.

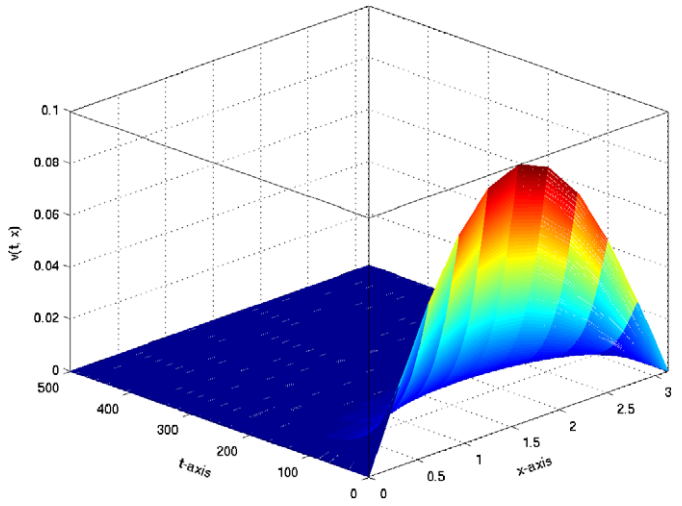

Fig. 6. Profile of $v(t, x)$ for $\lambda = 0.0105$, $\kappa = 0.01$, $\tau = 1$ and $T = 500$.

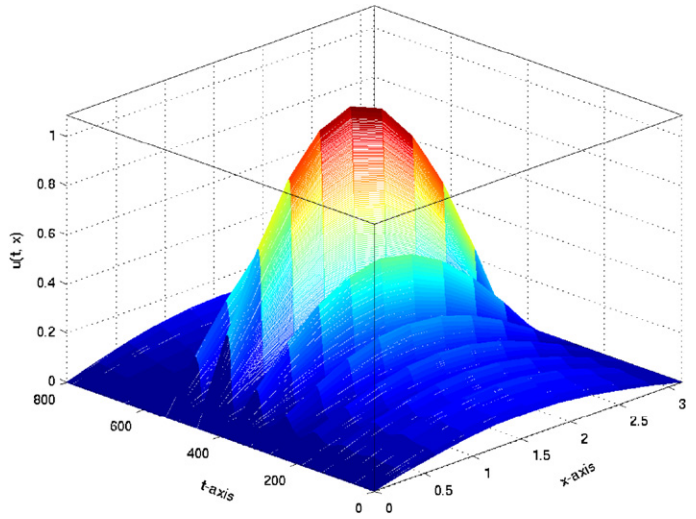

Fig. 7. Profile of $u(t, x)$ for $\lambda = 0.0097$, $\kappa = 0.01$, $\tau = 20$ and $T = 800$.

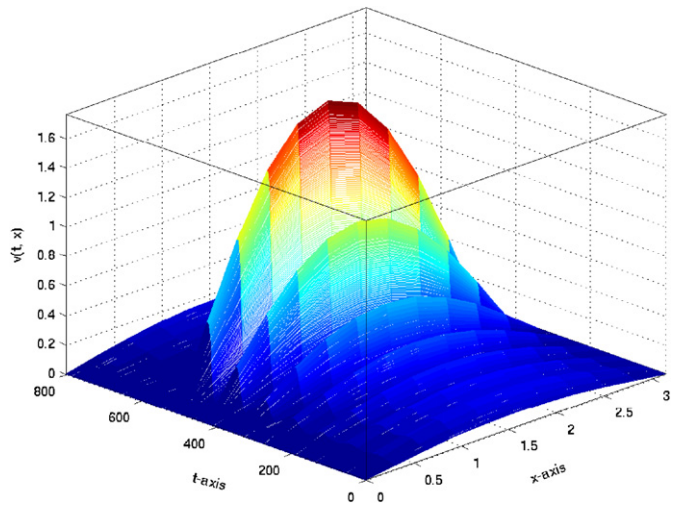

Fig. 8. Profile of $v(t, x)$ for $\lambda = 0.0097$, $\kappa = 0.01$, $\tau = 20$ and $T = 800$.

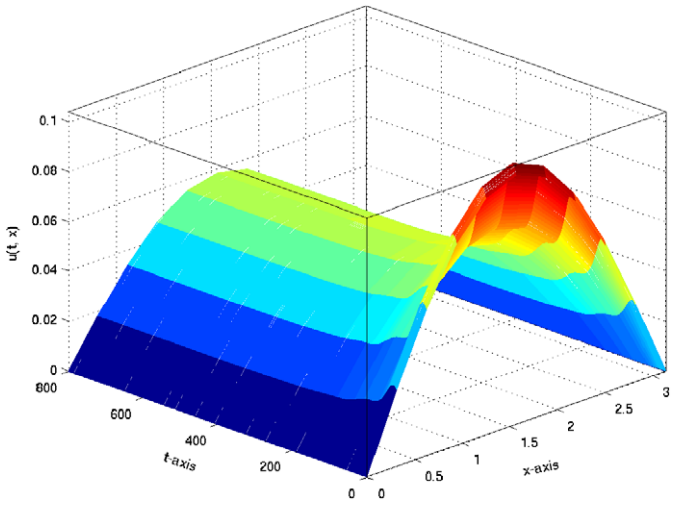

Fig. 9. Profile of $u(t, x)$ for $\lambda = 0.0098$, $\kappa = 0.01$, $\tau = 20$ and $T = 800$.

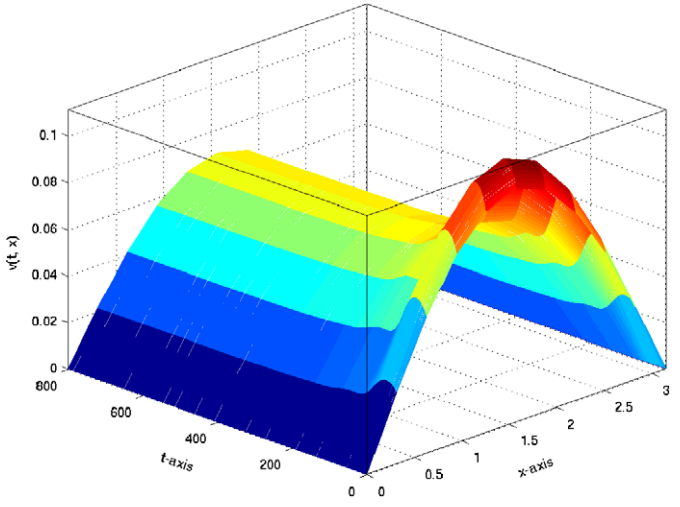

Fig. 10. Profile of $v(t, x)$ for $\lambda = 0.0098$, $\kappa = 0.01$, $\tau = 20$ and $T = 800$.

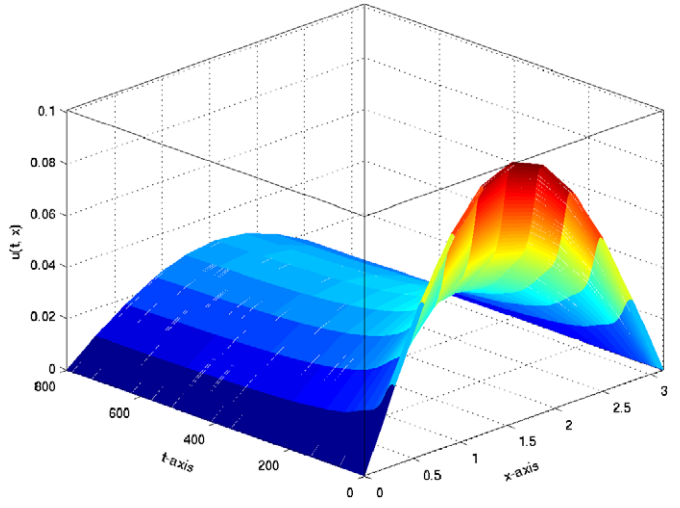

Fig. 11. Profile of $u(t, x)$ for $\lambda = 0.0099$, $\kappa = 0.01$, $\tau = 20$ and $T = 800$.

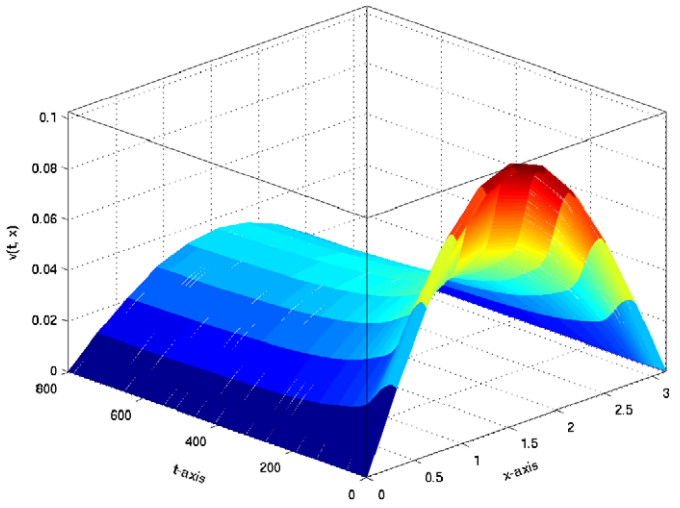

Fig. 12. Profile of $v(t, x)$ for $\lambda = 0.0099$, $\kappa = 0.01$, $\tau = 20$ and $T = 800$.

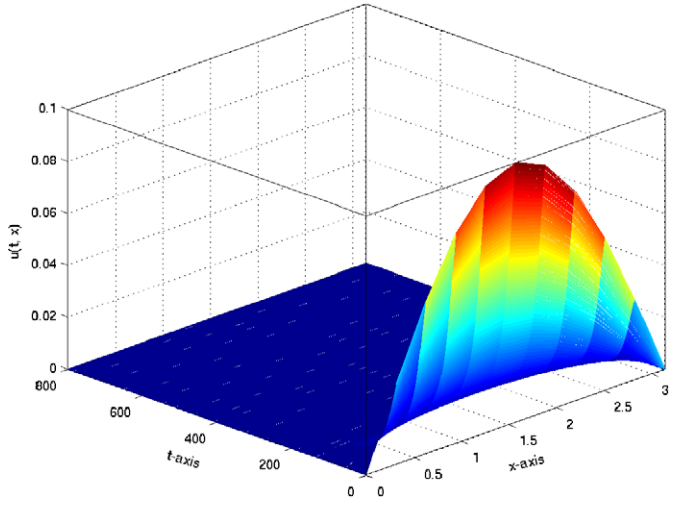

Fig. 13. Profile of $u(t, x)$ for $\lambda = 0.0105$, $\kappa = 0.01$, $\tau = 20$ and $T = 800$.

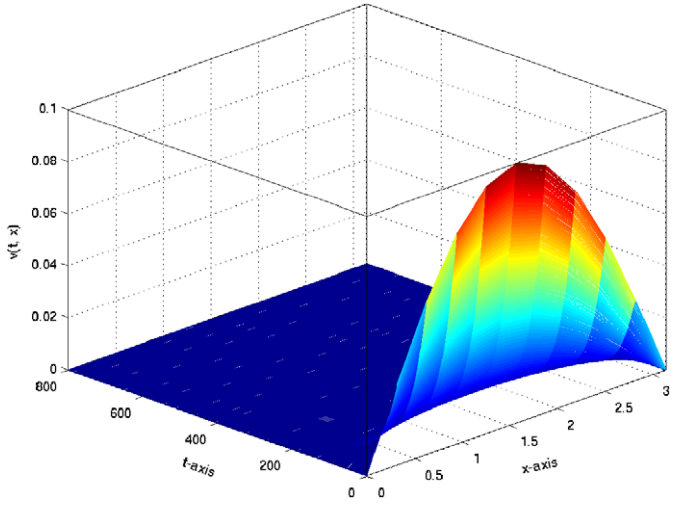

Fig. 14. Profile of $v(t, x)$ for $\lambda = 0.0105$, $\kappa = 0.01$, $\tau = 20$ and $T = 800$.

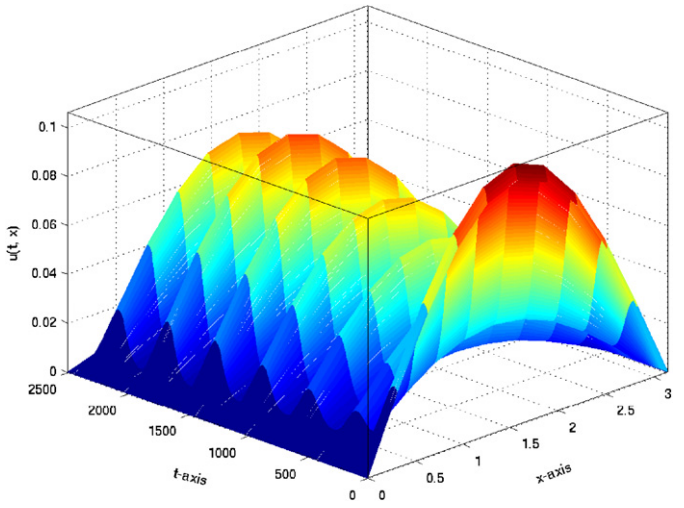

Fig. 15. Profile of $u(t, x)$ for $\lambda = 0.999$, $\kappa = 1.01$, $\tau = 100$ and $T = 2500$.

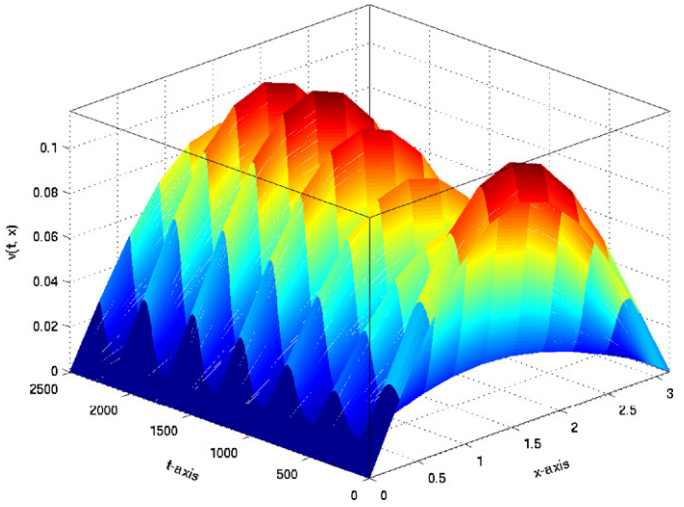

Fig. 16. Profile of $v(t, x)$ for $\lambda = 0.999$, $\kappa = 1.01$, $\tau = 100$ and $T = 2500$.

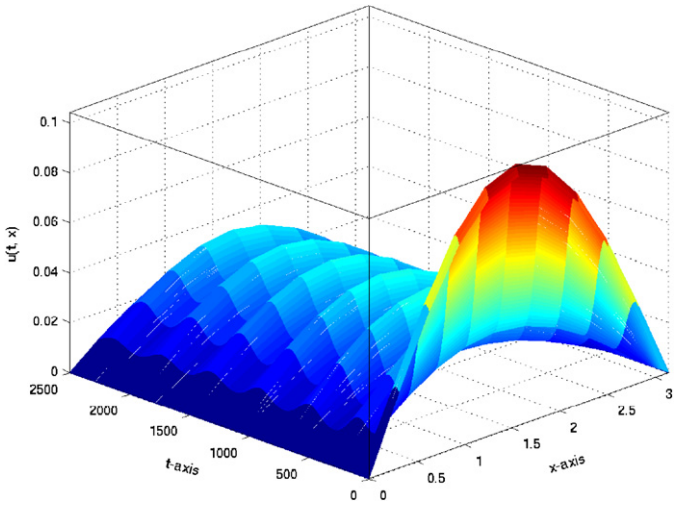

Fig. 17. Profile of $u(t, x)$ for $\lambda = 1.000$, $\kappa = 1.01$, $\tau = 100$ and $T = 2500$.

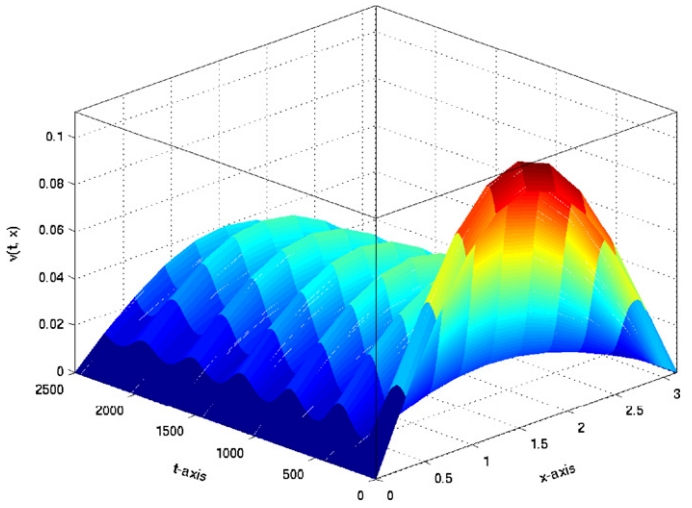

Fig. 18. Profile of $v(t, x)$ for $\lambda = 1.000$, $\kappa = 1.01$, $\tau = 100$ and $T = 2500$.

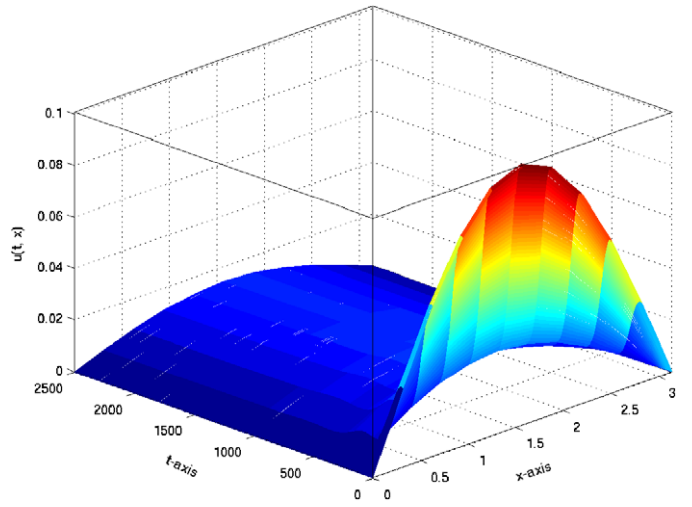

Fig. 19. Profile of $u(t, x)$ for $\lambda = 1.005$, $\kappa = 1.01$, $\tau = 100$ and $T = 2500$.

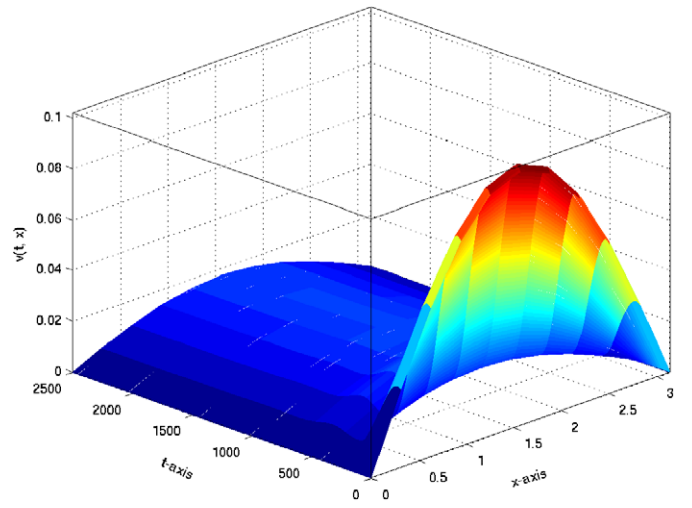

Fig. 20. Profile of $v(t, x)$ for $\lambda = 1.005$, $\kappa = 1.01$, $\tau = 100$ and $T = 2500$.

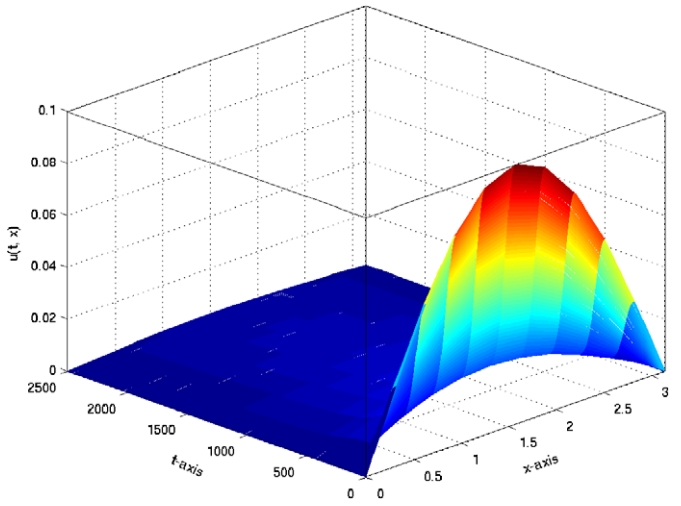

Fig. 21. Profile of $u(t, x)$ for $\lambda = 1.0105$, $\kappa = 1.01$, $\tau = 100$ and $T = 2500$.

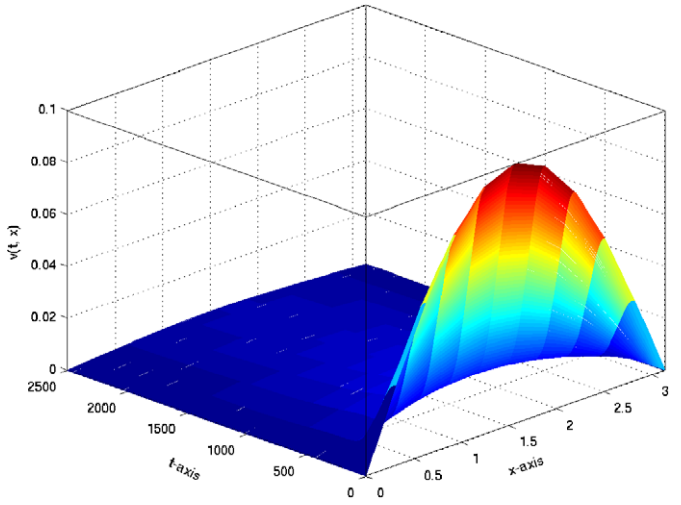

Fig. 22. Profile of $v(t, x)$ for $\lambda = 1.0105$, $\kappa = 1.01$, $\tau = 100$ and $T = 2500$.

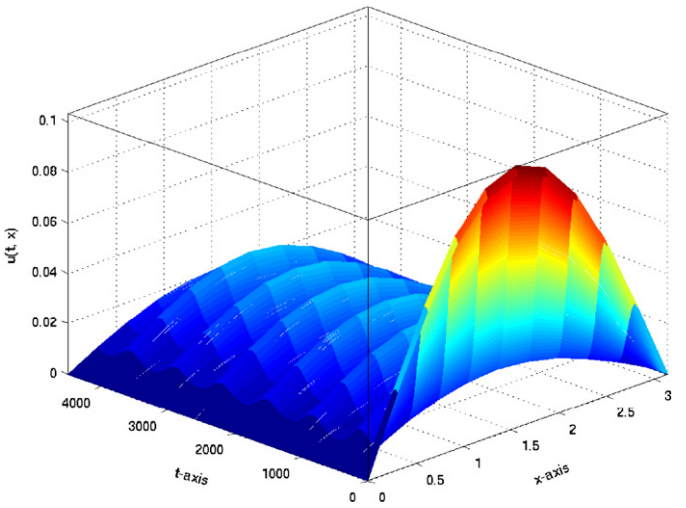

Fig. 23. Profile of $u(t, x)$ for $\lambda = 1.003$, $\kappa = 1.01$, $\tau = 170$ and $T = 4500$.

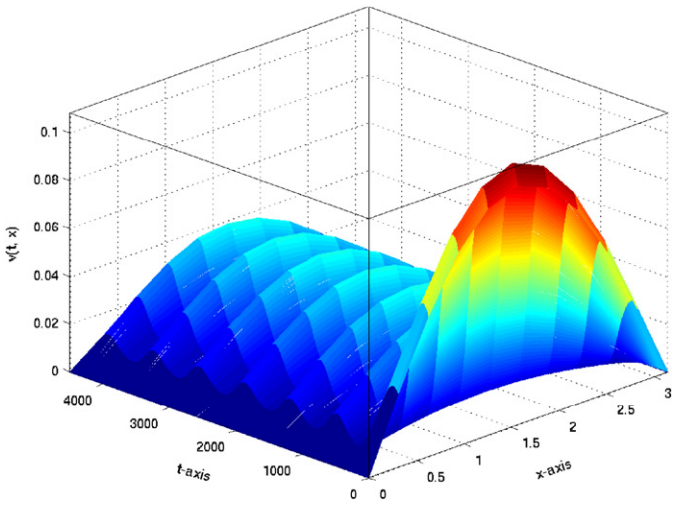

Fig. 24. Profile of $v(t, x)$ for $\lambda = 1.003$, $\kappa = 1.01$, $\tau = 170$ and $T = 4500$.

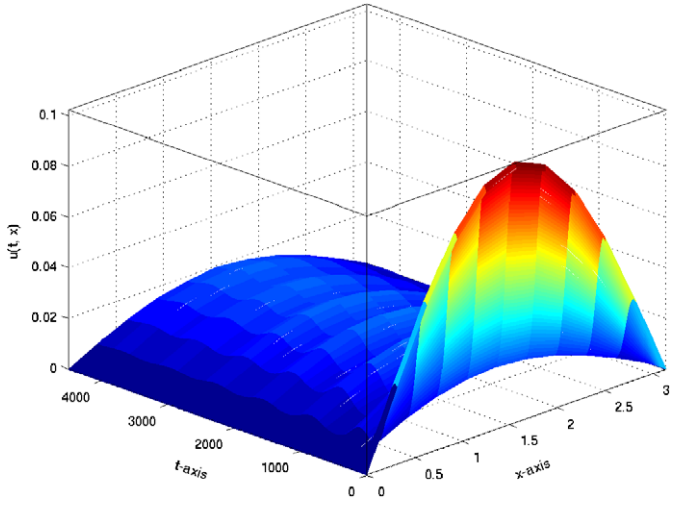

Fig. 25. Profile of $u(t, x)$ for $\lambda = 1.005$, $\kappa = 1.01$, $\tau = 170$ and $T = 4500$.

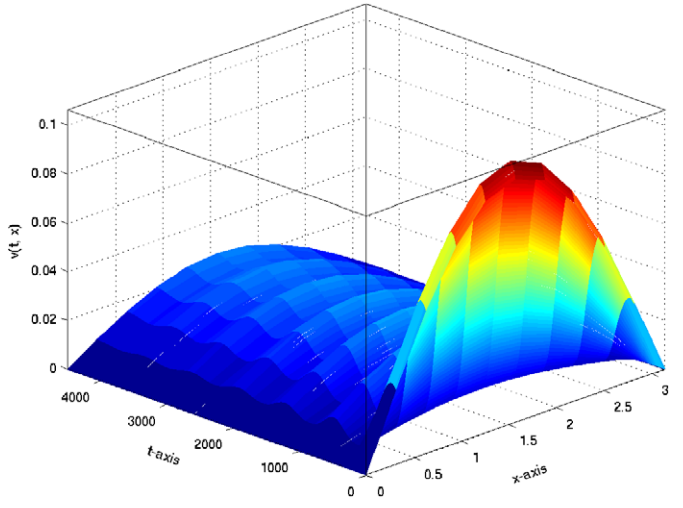

Fig. 26. Profile of $v(t, x)$ for $\lambda = 1.005$, $\kappa = 1.01$, $\tau = 170$ and $T = 4500$.

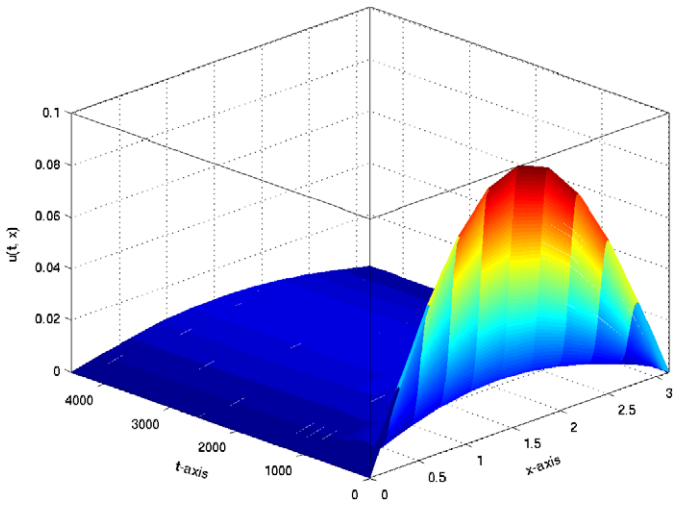

Fig. 27. Profile of $u(t, x)$ for $\lambda = 1.007$, $\kappa = 1.01$, $\tau = 170$ and $T = 4500$.

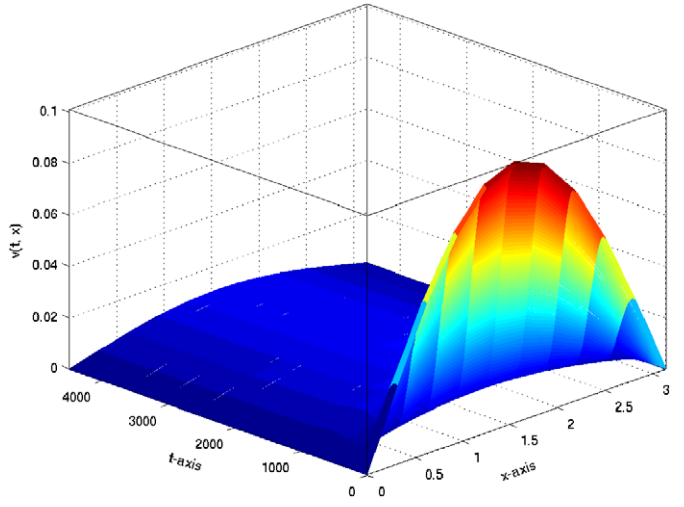

Fig. 28. Profile of $v(t, x)$ for $\lambda = 1.007$, $\kappa = 1.01$, $\tau = 170$ and $T = 4500$.

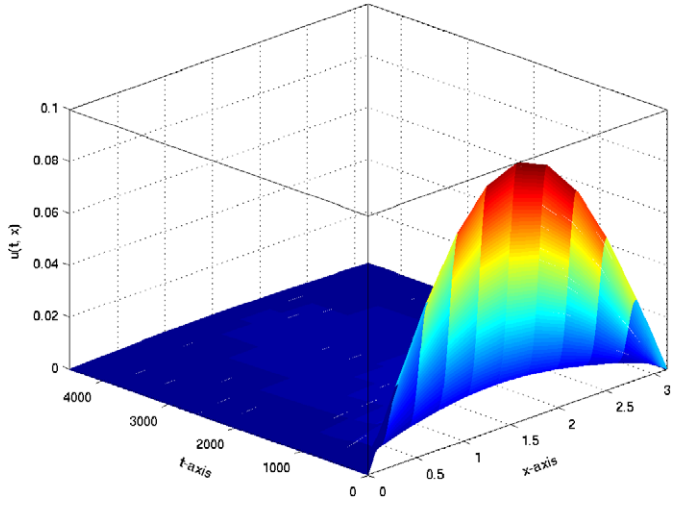

Fig. 29. Profile of $u(t, x)$ for $\lambda = 1.0105$, $\kappa = 1.01$, $\tau = 170$ and $T = 4500$.

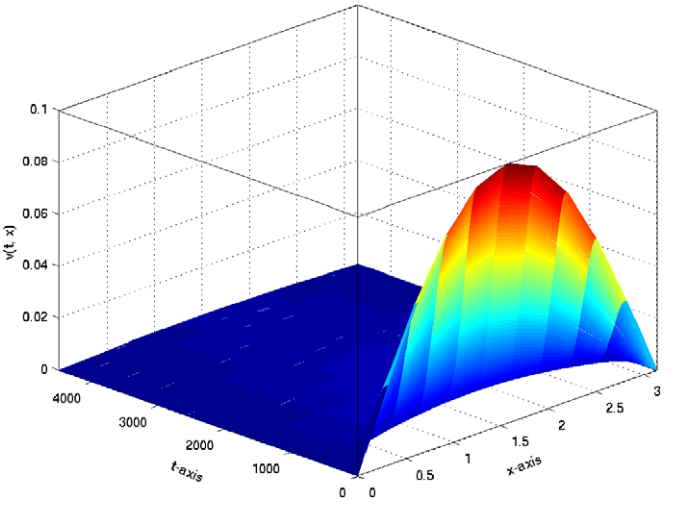

Fig. 30. Profile of $v(t, x)$ for $\lambda = 1.0105$, $\kappa = 1.01$, $\tau = 170$ and $T = 4500$.

- the ratio κ/λ is greater than 1 then there is a positive equilibrium and a positive real number $\kappa_1 \in (1, \kappa^\star)$ such that if $1 < \kappa/\lambda \leq \kappa_1$ then the positive equilibrium solution is stable, and if $\kappa/\lambda \in (\kappa_1, \kappa^\star]$ then it is unstable periodic or aperiodic.

Hence, these results that we have obtained by our FOFDM confirm the theory about the existence and stability of the positive equilibrium when $\tau > 0$ and $\kappa/\lambda > 1$. Moreover, our results are comparable to those obtained in [8] in which the authors solved problem (1.5)–(1.6) using the method of steps (where one transforms the DPDE into a system of ordinary PDEs) and the MATLAB PDE toolbox for $\tau = 20$, 100 and 170 and $T = 800$, 2500 and 4500. Their simulations show that the solution is stable for $\kappa/\lambda = 0.98$ and tends to the trivial attractor $(0, 0)$, when they took κ/λ as 1.01 and $\tau = 100$, a bifurcating periodic stable solution is noticed and finally when they took $\tau = 170$ and $\kappa/\lambda = 1.01$ they obtained an unstable Hopf bifurcating solution.

Another remarkable fact is that we have tested the MATLAB dde23 solver for solving the transformed system of DDEs and the dde23 could solve the problem for the delay $\tau = 20$ and $T = 800$ but it failed to solve the system for $\tau = 100$ and $\tau = 170$ on the domains $[0, T]$ with $T = 2500$ and $T = 4500$. The dde23 solved the problem using 12 371 grid points and consumed 70.02 s to compute the solution. On the other hand, our FOFDM solved the same problem using 3000 grid points and consumed 2.95 s to compute the solution. It is worth mentioning here that basically our method is able to produce a reliable solution to the problem with less number of grid points and in fairly less CPU time as compared to other in-built solvers.

Lastly, to avoid technicalities, we have considered the case when both diffusion coefficients λ_1 and λ_2 are the same. However, our approach can be extended for the general cases (for instance problem (1.1)–(1.2)) where $\lambda_1 \neq \lambda_2$ with necessary modifications. Currently, we are working on extending this approach to the model of two competitive species.

References

[1] L. Zhou, Y. Tang, S. Hussein, Stability and Hopf bifurcation for a delay competition diffusion system, Chaos, Solitons and Fractals 14 (2002) 1201–1225.
[2] J.D. Murray, Mathematical Biology I: An Introduction, third ed., Springer-Verlag, Berlin, 2001.
[3] J.D. Murray, Mathematical Biology II: Spatial Models and Biomedical Applications, second ed., Springer-Verlag, Berlin, 1993.
[4] A. Deutsch, R.B. de la Parra, R.J. de Boer, O. Diekmann, P. Jagers, E. Kisdi, M. Kretzschmar, P. Lansky, H. Metz, Mathematical Modeling of Biological Systems, vol. II, Birkhäuser, Boston, 2008.
[5] J. Mahaffy, J. Bélair, M.C. Mackey, Hematopoietic model with moving boundary condition and state dependent delay applications in Erythropoiesis, Journal of Theoretical Biology 190 (1998) 135–146.
[6] S. Panunzi, P. Palumbo, A. De Gaetano, A discrete single delay model for the intra-venous Glucose tolerance test, Theoretical Biology and Medical Modelling 4 (2007) 35.
[7] M. Villasana, A. Radunskaya, A delay differential equation model for tumor growth, Journal of Mathematical Biology 47 (2003) 270–294.
[8] W. Li, X. Yan, C. Zhang, Stability and Hopf bifurcation for a delayed cooperation diffusion system with Dirichlet boundary conditions, Chaos, Solitons and Fractals 38 (2008) 227–237.
[9] J.C. Butcher, Implicit Runge–Kutta processes, Mathematics of Computation 18 (85) (1964) 50–64.
[10] M.H. Holmes, Introduction to Numerical Methods Differential Equations, Springer, New York, 2007.
[11] R.M.M. Mattheij, S.W. Rienstra, J.H.M. ten Thije Boonkkamp, Partial Differential Equations, SIAM, Philadelphia, 2005.
[12] R.E. Mickens, Advances in the Applications of Nonstandard Finite Difference Schemes, World Scientific, Singapore, 2005.
[13] K.C. Patidar, On the use of nonstandard finite difference methods, Journal of Difference Equations and Applications 11 (8) (2005) 735–758.
[14] K.C. Patidar, K.K. Sharma, Uniformly convergent nonstandard finite difference methods for singularly perturbed differential difference equations with delay and advance, International Journal for Numerical Methods in Engineering 66 (2006) 272–296.
[15] K.C. Patidar, K.K. Sharma, ε-uniformly convergent non-standard finite difference methods for singularly perturbed differential difference equations with small delay, Applied Mathematics and Computation 175 (2006) 864–890.

[16] K.C. Patidar, A robust fitted operator finite difference method for a two-parameter singular perturbation problem, Journal of Difference Equations and Applications 14 (12) (2008) 1197–1214.
[17] S. Busenberg, W. Huang, Stability and Hopf bifurcation for a population model with diffusion effects, Journal of Differential Equations 124 (1996) 80–107.
[18] R.E. Mickens, Nonstandard Finite Difference Models of Differential Equations, World Scientific, Singapore, 1994.
[19] K.W. Morton, D.F. Mayers, Numerical Solution of Partial Differential Equations, Cambridge University Press, 2005.
[20] R.D. Richtmyer, K.W. Morton, Difference Methods for Initial-Value Problems, Interscience, New York, 1967.